Single-Molecule Investigation of Energy Dynamics in a Coupled Plasmon-Exciton System

Hiroshi Imada,[1] Kuniyuki Miwa,[1] Miyabi Imai-Imada,[1,2] Shota Kawahara,[1,2] Kensuke Kimura,[1,2] and Yousoo Kim[1,*]
[1]Surface and Interface Science Laboratory, RIKEN, 2-1 Hirosawa, Wako, Saitama 351-0198, Japan
[2]Department of Advanced Materials Science, Graduate School of Frontier Science, The University of Tokyo, 5-1-5 Kashiwanoha, Kashiwa, Chiba 277-8651, Japan
(Received 15 February 2017; published 5 July 2017)

We investigate the near-field interaction between an isolated free-base phthalocyanine molecule and a plasmon localized in the gap between an NaCl-covered Ag(111) surface and the tip apex of a scanning tunneling microscope. When the tip is located in the close proximity of the molecule, asymmetric dips emerge in the broad luminescence spectrum of the plasmon generated by the tunneling current. The origin of the dips is explained by energy transfer between the plasmon and molecular excitons and a quantum mechanical interference effect, where molecular vibrations provide additional degrees of freedom in the dynamic process.

DOI: 10.1103/PhysRevLett.119.013901

The electromagnetic field of localized plasmons around a metal nanostructure has a characteristic spatial distribution, polarization, and field gradient [1–7]. In contrast to the visible light propagating in a free-space with a wavelength of hundreds of nanometers, the plasmonic field of the same frequency can be localized down to ~1 nm. Precise understanding of plasmon-matter interactions, especially its spatial dependence, is highly required for further applications of plasmonics in ultrasensitive sensors, spectroscopic techniques, and energy-conversion devices. However, the nanoscale spatial features in the plasmon-matter interaction are still unclear because of the limited spatial resolution of conventional optical methods.

Scanning tunneling luminescence (STL) spectroscopy, where luminescence is induced by the injection of electrons from the tip of a scanning tunneling microscope (STM), provides a unique tool to investigate optical properties of matters with atomic scale precision [8–19]. A previous STL experiment study reported that the energy of the localized plasmon in the tunneling junction of an STM is absorbed by molecules located close to the STM tip [20]. Although the molecules were not visualized by STM in the study because the molecules were deposited on the shank of the STM tip, it was shown that molecular excitation by a plasmon (not by tunneling electron injection) is possible in the STM configuration. Theoretical investigations of plasmon-matter interaction show that energy transfer (absorption and emission) and interference effects can drastically modify the optical response of the coupled systems [21–26]. These pioneering works imply that the plasmon-molecule interaction can be investigated with an unprecedented precision if the near-field excitation of molecules by a localized plasmon and the capability of the STM to visualize individual molecular orbitals are successfully combined.

Here, we provide a precise description of the near-field interaction between a localized plasmon and a single molecule. The gap plasmon localized in the STM tunneling junction is used as a spatially controllable plasmonic probe driven by the tunneling current, and detailed STL measurements in the proximity of a free-base phthalocyanine (H_2Pc) molecule are performed. It is shown that even a single molecule modifies the optical property of the system to form "asymmetric dip" structures in the broad luminescence spectrum of the localized plasmon. Spectral analysis based on the quantum many-body theory [23,24] clarifies that the dip structures originate from energy transfer between the localized plasmon and molecular excitons. The spatial dependency of the spectroscopic signals in combination with the orbital visualization with STM reveals an anisotropic plasmon-exciton coupling through a radially polarized plasmonic field.

All experiments were performed with a low-temperature STM (Omicron) operating at 4.6 K under ultrahigh vacuum (UHV). Preparation of the sample and silver tips and experimental setup are described elsewhere [18]. H_2Pc was deposited onto the NaCl-covered Ag(111) at 4.7–10 K cooled in the STM head using an evaporator heated to 675 K. The STM stage was designed to be equipped with two optical lenses. The emitted light was collimated with the lens and directed out of the UHV chamber, where it was refocused onto a grating spectrometer (Acton, SpectraPro 2300i) with a photon detector (Princeton, Spec10) cooled with liquid nitrogen. All the optical spectra (except for Figs. S6 and S7 in the Supplemental Material [27]) were measured using a grating with 300 gr/mm. The STL spectra are not corrected for the optical throughput of the detection system.

Figure 1(a) illustrates the design of the experiment to investigate the detail of the near-field interaction between the localized plasmon and molecular excitons. The tunneling current of the STM generates the plasmon localized in the gap between the NaCl-covered Ag(111) surface and the Ag STM tip [29,30]. The plasmon then interacts with the molecule through the plasmon-exciton coupling, and the photons emitted from this coupled system are detected. The strength of the plasmon-exciton coupling is fine-tuned by changing the lateral distance between the molecule

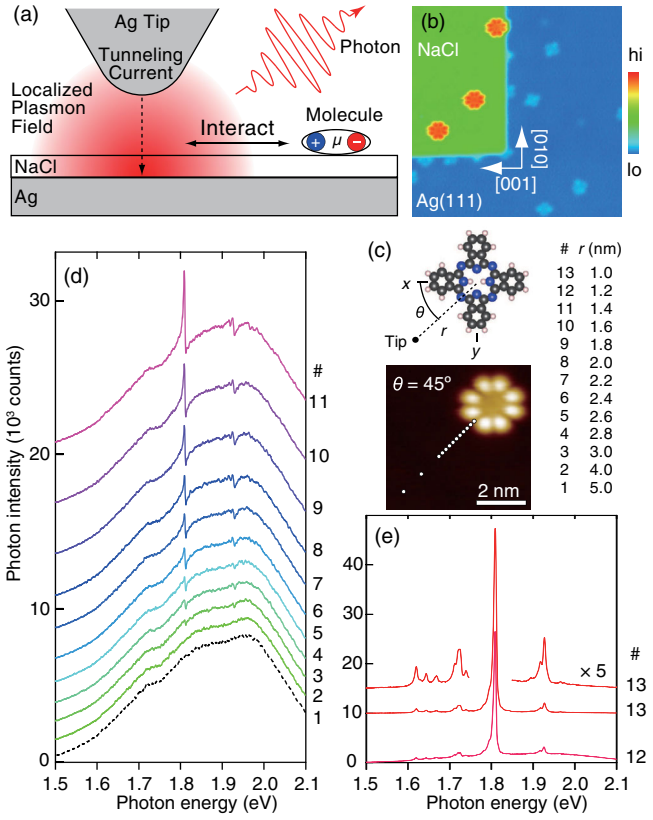

FIG. 1. Emergence of "dip" structures in STL spectra. (a) A schematic illustration of the experiment. μ represents the transition dipole moment of H_2Pc, which is oriented in the molecular plane. (b) An STM topographic image of H_2Pcs adsorbed on a three monolayer-thick NaCl(100) island grown on Ag(111) (sample bias voltage $V = -2.5$ V, tunneling current $I = 2$ pA, 25×25 nm^2). (c) The measurement tip positions for the spectra shown in (d) and (e) and the definition of the coordinates around the molecule. An H_2Pc (gray: C, blue: N, white: H) has two hydrogen atoms with a *trans* configuration at the molecular center. We follow the conventional definition of the molecular axes x and y, (x axis: parallel to N–H H–N bond) [32]. θ is measured from the x axis of H_2Pc. The column on the right is the list of the distances r measured from the molecular center. (d), (e) a series of STL spectra measured on and near an H_2Pc/NaCl with different tip positions on the NaCl film ($V = -2.3$ V,$I = 50$ pA, exposure time $t = 3$ min). The spectra are offset for clarity. A theoretical simulation corresponding to (d) is given in Fig. S2.

and the location of the localized plasmon with angstrom precision.

Figure 1(b) shows a topographic image of the sample. Since the electronic decoupling of a molecule from a metallic substrate is necessary to measure the intrinsic optical properties of the molecule [11], H_2Pc was deposited on an ultrathin NaCl(100) film [31] grown on Ag(111) (see Fig. S1 for the results of scanning tunneling spectroscopy). We define the coordinates around the molecule in Fig. 1(c).

A series of luminescence spectra induced by the tunneling current were obtained near an H_2Pc/NaCl as a function of the lateral distance of the STM tip from the molecular center [Figs. 1(d) and 1(e)]. When the tip is placed far from the molecule ($r \geq 4$ nm, # 1, 2), the luminescence spectrum is dominated by a broadband emission, which is attributed to the radiative decay of the localized plasmon [9]. Remarkably, dip structures emerge at 1.81 and 1.92 eV in the broad spectrum when the tip is positioned close to the molecule ($r = 1.4$–3 nm, # 3–11), and the spectral features becomes prominent as the tip is closer to the molecule. When the STM tip reaches the edge of the molecule where the direct excitation of the molecule by carrier injection turns into a possible pathway, intensive molecular electroluminescence is observed [Fig. 1(e)] [17,18]. The luminescence peaks at 1.81 and 1.92 eV are attributed to transitions from the first and second singlet excited states of H_2Pc, so-called the Q_x and the Q_y states [32–35], respectively. The small peaks at 1.60–1.75 eV are the vibronic satellites of the transition from the Q_x state (peak assignment is given in Fig. S3).

When the STM tip is located close to but outside of the molecule (#3–11), the molecule is not directly excited by charge injection. Hence, the emergence of the dips is attributed to the electromagnetic interaction between the molecular excitons and the localized plasmon that is generated by the inelastic tunneling current [9]. Figure 2(a) shows two representative STL spectra measured with tip positions far from and close to the molecule. We define the STL spectrum measured with the tip located far from the molecule as I_0 and that measured close to the molecule as $I(r, \theta)$. As shown in Fig. 2(b), the ratio spectrum I/I_0 clearly reveals the change in the spectral shape resulting from the plasmon-exciton coupling. The larger dip at 1.81 eV has an asymmetric feature, and the smaller dip at 1.92 eV has a more complex shape.

The origin of the dip structures is investigated based on the theory of STL using the nonequilibrium Green's function method [23,24] (see Supplemental Material [27]). Figure 2(c) shows calculated STL spectra with the plasmon-exciton coupling $\hbar g$ of 0 and 10 meV, and Fig. 2(d) displays the I/I_0 spectrum. STL spectra with and without the exciton-plasmon coupling term corresponds to the situations where the STM tip is located close to and far from the molecule, respectively. When $\hbar g = 10$ meV, the energy of localized plasmons is absorbed by the electronic transitions of the molecule through the plasmon-exciton coupling, which leads to the dip structures at 1.81 and 1.92 eV. The asymmetric spectral profile is explained by a quantum mechanical interference effect (Fano-like effect) [21,23,24,36] The energy of localized plasmons is absorbed by the molecule, and then the energy of the excited molecule is reemitted into localized plasmons. These processes interfere with each other, and the constructive and destructive interference of these processes leads to the enhancement and suppression of the energy transfer, resulting in asymmetric spectral shapes [23,24]. These dynamic processes in the coupled plasmon-exciton system are schematically summarized in Fig. 2(e). The energy of the localized plasmon is absorbed by the

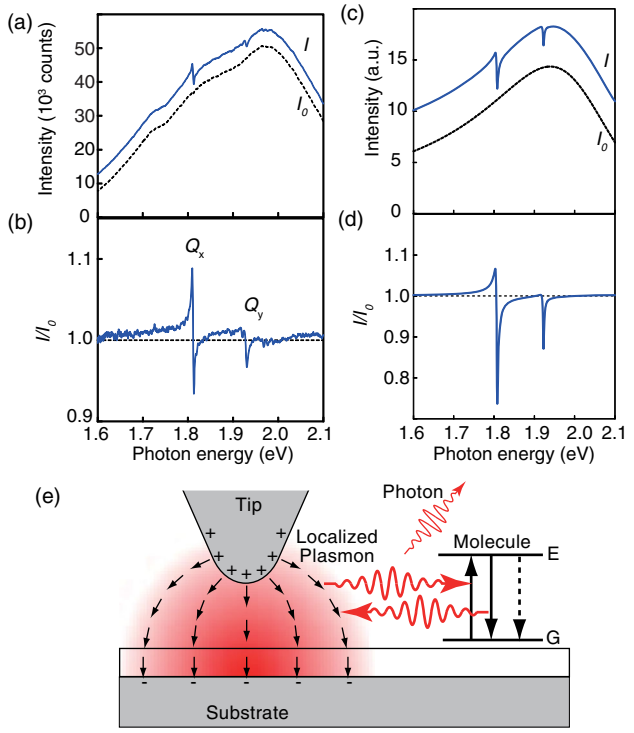

FIG. 2. Spectral analysis of the dip structures: comparison with theoretical calculations. (a) STL spectra measured on the NaCl film with $r = 2.2$ nm (upper) and 4 nm (lower) ($\theta = 45°$, $V = -2.5$ V, $I = 250$ pA,$t = 5$ min). (b) An $I(r,\theta)/I_0$ spectrum ($r = 2.2$ nm, $\theta = 45°$), generated by dividing the upper curve (I) with the lower curve (I_0) in (a). (c) Calculated luminescence spectra using the theory of STL [23,24] with plasmon-exciton coupling $\hbar g = 0$ (lower) and 10 meV (upper). Two molecular excited states with 1.81 and 1.92 eV are assumed. (d) An I/I_0 spectrum using the two simulated spectra in (c). (e) A schematic diagram illustrating the dynamic processes arising from the plasmon-exciton coupling. G and E stand for the ground and excited states of the molecule, respectively.

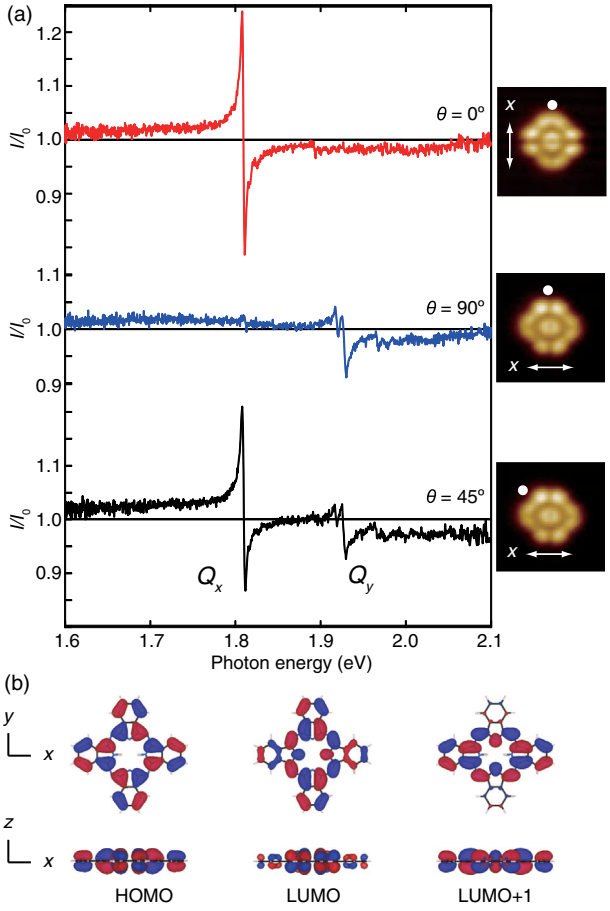

FIG. 3. Angle dependency in the plasmon-exciton coupling. $I(r,\theta)/I_0$ spectra measured at $\theta = 0°$, 45°, 90°, and $r = 1.6$ nm ($V = -2.2$ V,$I = 500$ pA,$t = 5$ sec, averaged 50 spectra). The corresponding STM images were obtained with $V = 0.6$ V and $I = 5$ pA. (b) Calculated molecular orbitals (HOMO, LUMO, and LUMO + 1) of H_2Pc in the gas phase. The calculations were performed with Gaussian09. The color (red or blue) represents the sign of the phase of the wave function. While HOMO is an odd function both in x and y, LUMO (LUMO + 1) is odd in x (y) but even in y (x). All the three MOs are odd in z.

molecule (upward arrow), and then the energy is reemitted into plasmons (downward solid arrow) or the energy is nonradiatively dissipated (downward dashed arrow).

Figure 3(a) shows the θ dependence of the absorption signal [θ is defined in Fig. 1(c)]. When the STM tip is on the x axis ($\theta = 0°$), the spectrum shows only one large dip at 1.81 eV (the Q_x state). Additionally, several small dips are found around 1.90 eV, which will be discussed later. When $\theta = 90°$, the Q_x dips disappear, and the spectrum displays only the Q_y dips around 1.92 eV with a rather complicated dip structure. The congested spectral feature has been explained by state mixing between the Q_y state and vibrationally excited Q_x state [33–35]. If the tip is placed between the x and y axes ($\theta = 45°$), both the Q_x and Q_y dips appear.

The clear separation of the Q_x and Q_y signals depending on θ reveals how the molecular excitons are coupled with the localized plasmon. The STM observation confirms that H_2Pc adsorbs with the molecular plane parallel to the surface, and the transition dipole moments (TDMs) $\vec{\mu}$ of H_2Pc associated with the Q_x and Q_y states are parallel to the molecular plane and polarized in x and y directions, respectively [32,33]. Therefore the plasmon-exciton coupling should be mediated by the horizontal component of the electric field $\vec{E}_{\parallel}(\omega)$ of the localized plasmon [37,38]. While $\vec{E}_{\parallel}(\omega)$ consists of radial and angular components, $\vec{E}_{\parallel}(\omega) = \vec{E}_r(\omega) + \vec{E}_\theta(\omega)$, the angular component $\vec{E}_\theta(\omega)$ is zero with an axially symmetric STM tip, or negligibly small in the reality of a slightly asymmetric tip, and $\vec{E}_{\parallel}(\omega)$ should be predominantly polarized in the radial direction $\vec{E}_{\parallel}(\omega) \approx \vec{E}_r(\omega)$. Therefore, when $\theta = 0°$ (90°), the radially polarized electric field of the localized plasmon aligns parallel with the direction of the TDM of the Q_x (Q_y) state, and the Q_x and Q_y can be selectively excited depending on

the tip position. Based on these considerations, it can be concluded that the localized plasmon as an excitation source provides us a unique way to determine the direction of a TDM. From the other viewpoint, the single molecule can be regarded as a local probe of the strength and polarization of the plasmonic field, enabling a visualization of its spatial distribution.

Real-space characterization of local excited states as demonstrated here is not feasible with usual STM techniques because of the short lifetime of the excited states. This capability is particularly valuable, because, energy levels of a molecule at the excited state are not directly deduced from those at the ground state, and this is also a nontrivial issue even for sophisticated first principles calculations [32]. Based on the energy levels of the ground state of H_2Pc, the electronic transition between the highest occupied molecular orbital (HOMO) and lowest unoccupied molecular orbital (LUMO) seems to contribute to the first singlet excited state and the HOMO − LUMO + 1 transition to the second singlet excited state. However, previous studies of H_2Pc have determined that the HOMO–LUMO (HOMO − LUMO + 1) transition is the major component of the second (first) singlet excited state, inversely [32]. This remarkable assignment is consistent with our results. As shown in Fig. 3(a), the second singlet excited state (Q_y) is exclusively detected when the direction of $\vec{E}_{\parallel}(\omega)$ is aligned with the y axis of H_2Pc ($\theta = 90°$), in which only the electric dipole transition between the HOMO and LUMO is allowed by the selection rule. In addition, the HOMO–LUMO transition in the x direction is prohibited by the selection rule. This is because both MOs have the same (odd) parity in x [Fig. 3(b)], and the Q_y state is never detected when $\vec{E}_{\parallel}(\omega)$ is aligned with the x axis ($\theta = 0°$).

Finally, we analyze fine structures in the I/I_0 spectrum. Figure 4(a) shows an I/I_0 spectrum of the Q_x state with a better signal-to-noise ratio. In addition to the large asymmetric dip at 1.81 eV, small dips and peaks are observed on the higher- and lower-energy sides, respectively. By subtracting the large asymmetric component from the interfering 0-0 transition, the fine structures are clearly revealed [lower curve in Fig. 4(a)]. Reminiscent of the mirror symmetry between absorption and emission spectra [35], the dips and peaks are located at symmetric positions with respect to the band origin of the Q_x state (1.81 eV). The peaks below 1.81 eV match with the vibronic satellites in the STL electroluminescence [Fig. 1(e) and Fig. S3] and photoluminescence spectra [35], showing that they originate from luminescence of the Q_x state. The dips above 1.81 eV agrees well with the polarization-sensitive fluorescence excitation spectrum of H_2Pc in the solid Ar matrix [33], indicating that they originate from the energy absorption by the Q_x state. More detailed assignment of the peaks and dips are discussed in the Supplemental Material (Fig. S4) [27].

The state transitions observed in the I/I_0 spectrum are summarized in the energy diagram [Fig. 4(b)]: interfering energy absorption and emission at 1.81 eV, transitions from

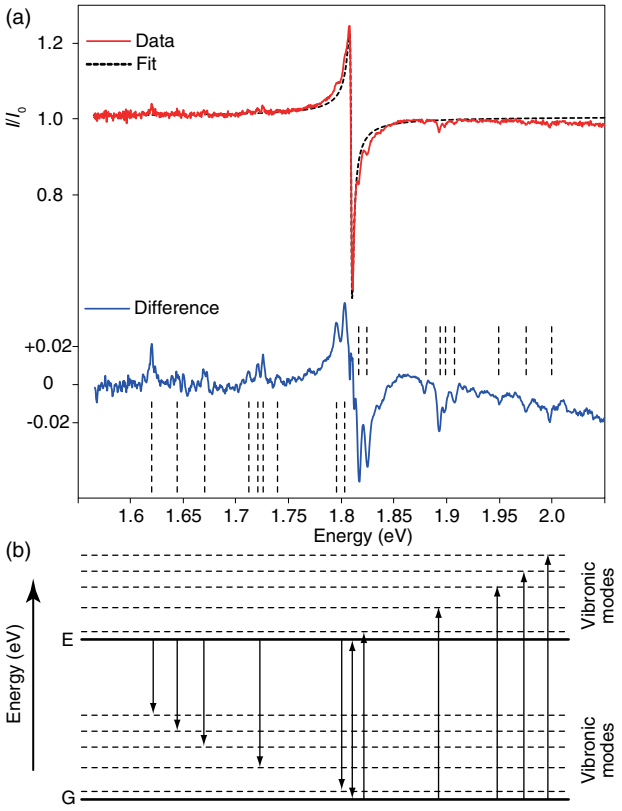

FIG. 4. Fine structures in I/I_0 spectrum. (a) The same measurement as the top curve in Fig. 3(a) was performed with a different tip condition ($r = 1.8$ nm, $V = -2.2$ V, $I = 500$ pA, $t = 5$ sec, averaged 100 spectra). The experimental data were fitted with a single Breit-Wigner-Fano function and was subtracted by the fitted curve to give the lower curve. (b) An energy diagram summarizing the observed transitions. G, ground state; E, excited state.

the ground state to the vibrationally excited Q_x state (above 1.81 eV), and transitions from the vibrational ground state of the Q_x state to the vibrationally excited states of the electronic ground state (below 1.81 eV). Note that the molecular luminescence observed here was not induced by photon irradiation nor by electric current flowing through the molecule (the reason for neglecting the current flow is discussed in the Supplemental Material [27]). This is a novel molecular luminescence phenomenon induced purely by the localized plasmon, which can be called plasmoluminescence.

In conclusion, we have revealed the detailed coupling mechanism of the localized plasmon with a single-molecular exciton, which is mediated by the horizontal component of the radially polarized plasmonic field. We also have described the energy dynamics in the coupled plasmon-exciton-vibron system [23,24]. The reason why the dip formation was not observed in previous works [13,17,19] might be that the signal intensity measured outside the molecule is much weaker than that measured inside the molecule [Figs. 1(d) and 1(e) and Fig. S6]. Our results also

demonstrate that the use of the localized plasmon as a point excitation source enables us to determine the electronic and vibronic excitation energies of a single molecule and their polarization directions with a molecular scale spatial resolution. As shown in Fig. S7, the energy of the localized plasmon is tunable from the near-infrared to the visible range; thus, our methodology is expected to be widely applicable to various molecules, clusters, and local defects, even including nonluminescent objects. More importantly, our findings pave the way for establishing an absorption and emission spectroscopy with the ultimate sensitivity and spatial resolution, which will certainly expand our perception into fundamental energetic processes taking place at the single-molecule level.

This work was supported in part by a Grant-in-Aid for Scientific Research (S) [Grant No. 21225001], Scientific Research (A) [Grant No. 15H02025], Research Activity Start-up [Grant No. 26886013], Grant-in-Aid for Young Scientists (B) [Grant No. 16K21623] and JSPS Fellows [Grant No. 15J03915] from the Ministry of Education, Culture, Sports, Science, and Technology (MEXT) of Japan. Some of the numerical computations presented here were performed using RICC and HOKUSAI systems at RIKEN. We thank Maki Kawai, Tetsuo Hanaguri, Atsuya Muranaka, Ryuichi Arafune, Norihiko Hayazawa, and Holly Walen for helpful discussions.

*Corresponding author.
ykim@riken.jp (Y.K.).

[1] S. Lal, S. Link, and N. J. Halas, Nano-optics from sensing to waveguiding, Nat. Photonics **1**, 641 (2007).
[2] S. Kawata, Y. Inouye, and P. Verma, Plasmonics for near-field nano-imaging and superlensing, Nat. Photonics **3**, 388 (2009).
[3] L. Novotny and N. van Hulst, Antennas for light, Nat. Photonics **5**, 83 (2011).
[4] K. L. Kelly, E. Coronado, L. L. Zhao, and G. C. Schatz, The optical properties of metal nanoparticles: The influence of size, shape, and dielectric environment, J. Phys. Chem. B **107**, 668 (2003).
[5] E. Prodan, C. Radloff, N. J. Halas, and P. Nordlander, A hybridization model for the plasmon response of complex nanostructures, Science **302**, 419 (2003).
[6] M. Yamaguchi, K. Nobusada, and T. Yatsui, Nonlinear optical response induced by a second-harmonic electric-field component concomitant with optical near-field excitation, Phys. Rev. A **92**, 043809 (2015).
[7] F. Benz *et al.*, Single-molecule optomechanics in "picocavities", Science **354**, 726 (2016).
[8] J. K. Gimzewski, B. Reihl, J. H. Coombs, and R. R. Schlittler, Photon emission with the scanning tunneling microscope, Z. Phys. B **72**, 497 (1988).
[9] R. Berndt, J. K. Gimzewski, and P. Johansson, Inelastic Tunneling Excitation of Tip-Induced Plasmon Modes on Noble-Metal Surfaces, Phys. Rev. Lett. **67**, 3796 (1991).
[10] R. Berndt, R. Gaisch, J. K. Gimzewski, B. Reihl, R. R. Schlittler, W. D. Schneider, and M. Tschudy, Photon emission at molecular resolution induced by a scanning tunneling microscope, Science **262**, 1425 (1993).
[11] X. H. Qiu, G. V. Nazin, and W. Ho, Vibrationally resolved fluorescence excited with submolecular precision, Science **299**, 542 (2003).
[12] Z. C. Dong *et al.*, Generation of molecular hot electroluminescence by resonant nanocavity plasmons, Nat. Photonics **4**, 50 (2010).
[13] C. Chen, P. Chu, C. A. Bobisch, D. L. Mills, and W. Ho, Viewing the Interior of a Single Molecule: Vibronically Resolved Photon Imaging at Submolecular Resolution, Phys. Rev. Lett. **105**, 217402 (2010).
[14] H. Imada, K. Miwa, J. Jung, K. T. Shimizu, N. Yamamoto, and Y. Kim, Atomic-scale luminescence measurement and theoretical analysis unveiling electron energy dissipation at a *p*-type GaAs(110) surface, Nanotechnology **26**, 365402 (2015).
[15] P. Merino, C. Grosze, A. Roslawska, K. Kuhnke, and K. Kern, Exciton dynamics of C60-based single-photon emitters explored by Hanbury Brown–Twiss scanning tunnelling microscopy, Nat. Commun. **6**, 8461 (2015).
[16] M. C. Chong, G. Reecht, H. Bulou, A. Boeglin, F. Scheurer, F. Mathevet, and G. Schull, Narrow-Line Single-Molecule Transducer between Electronic Circuits and Surface Plasmons, Phys. Rev. Lett. **116**, 036802 (2016).
[17] Y. Zhang *et al.*, Visualizing coherent intermolecular dipole–dipole coupling in real space, Nature (London) **531**, 623 (2016).
[18] H. Imada, K. Miwa, M. Imai-Imada, S. Kawahara, K. Kimura, and Y. Kim, Real-space investigation of energy transfer in heterogeneous molecular dimers, Nature (London) **538**, 364 (2016).
[19] T. Lutz, C. Große, C. Dette, A. Kabakchiev, F. Schramm, M. Ruben, R. Gutzler, K. Kuhnke, U. Schlickum, and K. Kern, Molecular orbital gates for plasmon excitation, Nano Lett. **13**, 2846 (2013).
[20] N. L. Schneider and R. Berndt, Plasmonic excitation of light emission and absorption by porphyrine molecules in a scanning tunneling microscope, Phys. Rev. B **86**, 035445 (2012).
[21] A. Manjavacas, F. J. G. d. Abajo, and P. Nordlander, Quantum plexcitonics: strongly interacting plasmons and excitons, Nano Lett. **11**, 2318 (2011).
[22] H. Ishihara, A. Nobuhiro, M. Nakatani, and Y. Mizumoto, Anomalous optical response of metal–molecule coupled system, J. Photochem. Photobiol. A **221**, 148 (2011).
[23] K. Miwa, M. Sakaue, and H. Kasai, Effects of interference between energy absorption processes of molecule and surface plasmons on light emission induced by scanning tunneling microscopy, J. Phys. Soc. Jpn. **82**, 124707 (2013).
[24] K. Miwa, M. Sakaue, B. Gumhalter, and H. Kasai, Effects of plasmon energetics on light emission induced by scanning tunneling microscopy, J. Phys. Condens. Matter **26**, 222001 (2014).
[25] X.-W. Chen, V. Sandoghdar, and M. Agio, Coherent Interaction of Light with a Metallic Structure Coupled to a Single Quantum Emitter: From Superabsorption to Cloaking, Phys. Rev. Lett. **110** (2013).

[26] M. Nakatani, A. Nobuhiro, N. Yokoshi, and H. Ishihara, Model of the photoexcitation processes of a two-level molecule coherently coupled to an optical antenna, Phys. Chem. Chem. Phys. **15**, 8144 (2013).

[27] See Supplemental Material at http://link.aps.org/supplemental/10.1103/PhysRevLett.119.013901 for a description on theoretical calculations, additional experimental data, and discussions, which include Ref. [28].

[28] G. Raunio, L. Almqvist, and R. Stedman, Phonon dispersion relations in NaCl, Phys. Rev. **178**, 1496 (1969).

[29] K. Amemiya, Light emission induced by a scanning tunnel microscope from a doubly layered substrate, Phys. Rev. B **67**, 075409 (2003).

[30] X. Tao, Z. C. Dong, J. L. Yang, Y. Luo, J. G. Hou, and J. Aizpurua, Influence of a dielectric layer on photon emission induced by a scanning tunneling microscope, J. Chem. Phys. **130**, 084706 (2009).

[31] J. Repp, G. Meyer, S. M. Stojković, A. Gourdon, and C. Joachim, Molecules on Insulating Films: Scanning-Tunneling Microscopy Imaging of Individual Molecular Orbitals, Phys. Rev. Lett. **94**, 026803 (2005).

[32] R. Fukuda, M. Ehara, and H. Nakatsuji, Excited states and electronic spectra of extended tetraazaporphyrins, J. Chem. Phys. **133**, 144316 (2010).

[33] V. E. Bondybey and J. H. English, Spectra of the H_2 phthalocyanine in low-temperature matrixes, J. Am. Chem. Soc. **101**, 3446 (1979).

[34] P. S. H. Fitch, C. A. Haynam, and D. H. Levy, The fluorescence excitation spectrum of free base phthalocyanine cooled in a supersonic free jet, J. Chem. Phys. **73**, 1064 (1980).

[35] C. Murray, N. Dozova, J. G. McCaffrey, N. Shafizadeh, W. Chin, M. Broquier, and C. Crepin, Visible luminescence spectroscopy of free-base and zinc phthalocyanines isolated in cryogenic matrices, Phys. Chem. Chem. Phys. **13**, 17543 (2011).

[36] I. Gerhardt, G. Wrigge, P. Bushev, G. Zumofen, M. Agio, R. Pfab, and V. Sandoghdar, Strong Extinction of a Laser Beam by a Single Molecule, Phys. Rev. Lett. **98**, 033601 (2007).

[37] D. L. Mills, Theory of STM-induced enhancement of dynamic dipole moments on crystal surfaces, Phys. Rev. B **65**, 125419 (2002).

[38] P. J. Schuck, W. Bao, and N. J. Borys, A polarizing situation: Taking an in-plane perspective for next-generation near-field studies, Front. Phys. **11**, 117804 (2016).